MICROCHANNEL PLATE WAFER IMAGE TUBE INTENSIFIED CHARGE-INJECTION DEVICE CAMERAS

C. B. Johnson, T. F. Lynch and J. J. Cuny*

ABSTRACT

Low-light-level television (LLLTV) camera performance is achieved by fiberoptically coupling a microchannel plate (MCP) wafer image intensifier to a silicon charge-injection device (CID) camera. Some of the performance characteristics of intensifier/CID (ICID) combinations can be predicted by using the model described in this paper before an ICID camera is made. The predicted performance using this model is compared to the specific ICID camera made using an ITT #F4111 MCP wafer image intensifier fiberoptically coupled to a 244 x 248 pixel GE CID. Good agreement between the predicted and measured performance characteristics is found. The ITT ICID camera has the following general characteristics: spectral response, S20; distortion, <1%; input light level threshold, 1E-5 lx; frame rate, 30 frames/s; dynamic range, 100/1.

INTRODUCTION

Image intensified SSA readout cameras have been discussed by several authors[1-4]. In this paper some theoretical and experimental properties of MCP wafer image tube intensified CIDs are discussed. These ICIDs are shown to have LLLTV camera characteristics that are competitive in some respects with SIT and ISIT camera tubes, except for the number of TV lines per picture height. This relative disadvantage of ICIDs will be reduced in the future when CIDs having more pixels are developed. However, even now the relative size, weight and power advantages of ICIDs make them preferred over SITs and ISITs for some applications. The generalized design of an ICID camera is shown schematically in fig.1. The input optical image is amplified and wavelength-converted by the MCP image tube, and the output image from this tube is fiberoptically coupled to the CID array. A video signal is produced by the CID camera electronics. The optical/electrical signal conversion processes in this camera is shown schematically in fig.2. An input optical image is focused through the window (W) and onto the photocathode (K) of the MCP wafer tube, and the resulting signal photoelectrons (e) are accelerated toward the MCP. These electrons emerge from the MCP, after receiving a total gain G, and they are accelerated toward the output phosphor screen (S). The fluorescence light from the screen is fiberoptically coupled to the CID array by the tube fiberoptic (FO') and the array fiberoptic (FO") windows, respectively.

ICID MODEL OF PERFORMANCE

Each medium, eg window, electron flow region, MCP, etc, used in an ICID camera has an effect on the output TV video signal produced at the camera output in response to an optical input. Figure 3 shows several of the different photo-response characteristics that are available in ICIDs. One of the main advantages of using a photocathode in place of silicon as the prime detector in any application is the difference in the relative spectral response of a photocathode with respect to silicon. Also, the use of a photocathode is required if either electron optical gain or operation in the ultraviolet (UV) spectral region is necessary. For example, only by some method, such as those described in this paper, where photon-to-photoelectron conversion occurs outside the CID itself, can single photon events be individually detected. The modulation transfer functions (MTFs) of the main image transfer and conversion sections are included in

*ITT/Electro-Optical Products Div, 3700 E Pontiac St,Ft Wayne IN 46803 USA

this model, and these MTFs are summarized in Table 1. Typical values for the parameters used in these MTF equations are also listed in Table 1. The MTF of a fiberoptic-input-window/cathode combination is given in Table 1A, where D_1 is the fiber diameter[5].

The photoelectrons which leave the cathode have an anisotropic energy distribution, and they are accelerated toward the MCP input electrode by the electric field in the K/G1 gap, as shown schematically in fig.2. The MTF of this image transfer process is given in Table 1B, using the equation derived by Eberhardt[6], where V_2 is the applied potential between the cathode and the MCP input electrode, $\overline{V}_{r2}$ is the average radial emission energy of the photoelectrons (assumed to be a Maxwellian energy distribution), and L_2 is the distance between the cathode and the MCP. One of the unique features of this cathode/MCP section is that a gate-pulse of about 200 V applied between the K and G1 electrodes can be used to electronically control the exposure period. This is found to be very useful for range-gating and ultra high-speed, eg several nanosecond, shutter tube applications[7,8].

Image tube technology has been revolutionized during the last decade by the development of microchannel plates. The manufacturing and performance characteristics of MCPs have been reviewed by Catchpole[9] and Lescovar[10], and significant development work on MCPs is still being accomplished. For our purposes, the necessary parameters relating to MCPs are gain and MTF. The current gain of an MCP is given by

$$G(V_3) = G_o V_3^m \qquad (1)$$

where V_3 is the potential applied across the MCP electrodes, G_o is the gain constant, and m is the gain index[11]. The MTF of the MCP is given in Table 1C, where D_3 is the MCP pore size.

The electron optical image transfer between the MCP and the phosphor screen is similar to that between the cathode and the MCP. However, the initial electron energy conditions and the interelectrode spacing are different. The MTF for this region is given in Table 1D, where V_4 is the MCP/screen applied potential, $\overline{V}_{r4}$ is the mean radial emission energy from the MCP, and L_4 is the MCP/screen spacing.

The cathode current density in the image tube is given by

$$J = SH\ , \qquad (2)$$

where S is the cathode white-light sensitivity (A/lm) and H is the faceplate illuminance (lx). For uniform cathode illuminance the total cathode current (I) is

$$I = \pi S H d_1^2/4 \qquad (3)$$

where d_1 is the cathode diameter. The total current density out of an MCP having a gain (G) is thus

$$J' = SHG, \qquad (4)$$

and the power density (P') into the phosphor screen is

$$P' = SHG(V_4 - V_d) \qquad (5)$$

where V_4 is the MCP/screen applied potential and V_d is the effective dead-potential of the screen. The spectral output photon flux (photons/m^2/s/nm), having the spectral distribution of the phosphor screen, is given by

$$f(\lambda) = SHG(V_4 - V_d)p(\lambda), \qquad (6)$$

where $p(\lambda)$ is the quantum yield factor (photons/eV/nm) for the phosphor screen. The total output photon flux is

$$F = \int_0^\infty f(\lambda)d\lambda = SHG(V_a - V_d)P, \qquad (7)$$

where $P = \int_0^\infty p(\lambda)d\lambda$. The gain of the image tube can therefore be expressed as

$$g = F/H = SG(V_4 - V_d)P, \qquad (8)$$

in units of photons/m^2/s/lx. The MTF of the phosphor screen is assumed to be the equation given ($T_5(f)$) in Table 1E, where the values of the

spatial frequency constant f_{c5} and the MTF index depend upon its thickness, the type of electrode employed, and the particle size distribution in the screen. The MTF of the fiberoptic window that the screen is deposited on is given in Table 1F, where D_6 is the fiber diameter. The Lambertian light transmission loss which occurs in the fiberoptic plate material used in our image tube

$$T' = \exp -L_6/\ell_6, \tag{9}$$

where L_6 is the length of the output window, and ℓ_6 is the absorption length. The shape of the spectral output distribution of a phosphor screen chosen to match to the SSA response is relatively unaffected by the fiberoptic material. We have used a type "Red #2" phosphor screen material and Galileo #D14EMA fiberoptic windows.

The method of joining the image intensifier tube to the CID is shown schematically in fig.1. A fiberoptic window is first bonded to the CID to form the readout assembly, and then this readout assembly is bonded to the output fiberoptic of the intensifier tube. This modular ICID design approach has the advantage that either the tube or the CID assembly can be easily replaced. The MTF loss at this tube/CID fiberoptic/fiberoptic interface is given by the equation in Table 1G, where D_7 is the fiber diameter size for the fiberoptic which is bonded to the CID, assuming intimate contact between these two fiberoptic windows. During its passage through the CID-fiberoptic window the signal light suffers its final transmission loss (T"), given by

$$T'' \simeq \exp -L_7/\ell_7, \tag{10}$$

where L_7 is the length of the CID fiberoptic window, and ℓ_7 is its absorption length. The final loss of MTF occurs at this fiberoptic/CID interface. Assuming that this fiberoptic and the CID are in intimate optical contact, these final vertical and horizontal direction MTFs are given in Table 1H, where D_8 is the center/center spacing between CID pixels in the vertical and horizontal directions, respectively. The spectral distribution for a "Red #2" phosphor screen of the type used in our ICID camera is shown in fig.4, along with the spectral sensitivity of the CID.

The total charge deposited within a pixel in a time period t is

$$Q(t) = tT'T''\alpha \int f(\lambda)Y(\lambda)d\lambda , \tag{11}$$

where α is the pixel area, and $Y(\lambda)$ is the absolute spectral yield of the CID (e/photon/nm). Alternatively, this equation can be rewritten as

$$Q(t) = tT'T''A_p F Y_{max} M, \tag{12}$$

where Y_{max} is the maximum absolute quantum yeild of the CID (e/photon). The parameter M is the spectral matching factor between the screen and the CID, given by

$$M = \int_0^\infty P(\lambda)y(\lambda)d\lambda \Big/ \int_0^\infty P(\lambda)d\lambda , \tag{13}$$

where $y(\lambda)$ is the relative spectral sensitivity of the CID. The maximum charge that can be stored in a pixel is

$$Q_s = C_p V_p, \tag{14}$$

approximately, where C_p is the pixel capacitance and V_p is the pixel bias potential. Thus, since $Q(t) \leq Q_s$, eqs.(7, 12, and 14) can be used to give the expression for the pixel saturation charge in terms of the ICID camera operating parameters:

$$tT'T''\alpha\, SHG(V_a - V_d)P\, Y_{max}\, M \leq C_p V_p, \tag{15}$$

For example, the maximum input faceplate irradiance is found to be H_{max} = 6E-3 lx for the following typical parameter values: C_p = 1 pF, V_p = 5 V, t = 33 ms, T' = 0.9, T" = 0.9, α = 36 x 46 μm^2, S = 190 μA/lm, G = 1000, V_a = 5500 V, V_d = 1500 V, P = 0.06 photons/eV, Y_{max} = 0.6 e/photon and M = 0.7.

ICID CAMERA CHARACTERISTICS

The CID type of imaging SSA was developed by Michon and Burke[12] in 1973. The latest CID camera (GE type #TN-2500) employs arrays having 244 x 248 pixels. This new camera has several additional features such as inject-inhibit-readout and automatic-gain-control. A general review of the design and readout options for CIDs is given by Burke and Michon[13].

The spectral response of our prototype ICID camera is approximately the same as the S20 curve shown in fig.3, and its white light (2854K, tungsten) sensitivity is 190 μA/lm. Since the quantum efficiency of the ICID camera is determined by the photocathode and window combination chosen for use in the image intensifier tube, the spectral range from the soft x-ray to the near-infrared can be reached directly by other ICID cameras of this type.

Electronic gating is easily and conveniently accomplished by dropping the potential of the G1 electrode in the image tube, see fig.1, to a value slightly lower than the potential of the cathode so that electrons cannot flow to the MCP and produce an output signal.

The "Red #2" phosphor screen used in the image tube yields a higher spectral matching factor value with the silicon CID than could be achieved using a P20 phosphor screen. The spectral matching factor of the spectral output from the "P20Red" phosphor screen and the CID spectral sensitivity ($Y(\lambda)$) is found to be 0.7.

The signal transfer characteristic of the ICID camera is shown in fig.5. The ICID camera detection capability is lower by a factor of 1E4 than its unintensified counterpart. The threshold of maximum sensitivity is adjustable by varying the gain of the image intensifier tube, and this is conveniently accomplished by changing the applied potential to the MCP in the tube. Figure 5 also shows that the ICID camera has a linear response (unity gamma) with a dynamic range of approximately 100/1.

The measured limiting visual resolution versus faceplate illuminance characteristic of the ICID is shown in fig.6. The LLL limiting resolution is determined by the faceplate irradiance, the quantum efficiency of the cathode, noise processes, and the exposure period. The high light level limiting resolution is set by the image transfer and conversion properties of all the components in the input-image/signal-output chain, as discussed earlier. The ICID maximum limiting resolution is 9 cycles/mm in both the vertical and horizontal directions, compared to the somewhat higher theoretical estimates given at the bottom of Table 1.

The maximum signal/noise ratio of the GE/#TN-2500 CID camera is 43 dB (peak-peak/rms) when operated under the normal TV scan conditions for this camera. With the MCP image intensifier tube fiberoptically coupled to the CID, there is no observable difference between the noise in the output video signal from the camera electronics when the tube is switched on and off, at room temperature ($\sim$23 ^{o}C), and when the tube is operating at the gain value which produced the signal-transfer curve shown in fig.5.

OTHER POSSIBLE ICID DESIGNS & ICID CAMERA APPLICATIONS

Other possible designs for ICID LLLTV cameras include the use of high-gain MCPs for photon-counting, multiple CIT readout of larger diameter image intensifier tubes with special fiberoptic couplers, the use of a proximity focused diode "pre-gain" image intensifier fiberoptically coupled to an MCP wafer image intensifier, and the use of special cathodes for spectral response reaching from the x-ray to the near-IR spectral regions. Possible applications of the ICID camera are those re-

quiring LLLTV surveillance, security/law-enforcement, x-ray cameras, space-borne-cameras for planetary-observations/astronomy, military TV cameras in aircraft, missiles, RPVs, etc.

SUMMARY AND CONCLUSIONS

The main image transfer and conversion processes in a proximity-focused microchannel-plate image-intensified charge-injection device (ICID) camera have been utilized to develop a model of its performance. Results from a prototype ICID camera, shown in fig.7, have been obtained, and it is found that the model agrees, within experimental error, with some of these results. Additional ICID measurements are being made. The ICID camera is a good sensor choice for LLLTV applications where its 1E-5 ℓx limit of sensitivity (at 30 frames/s), its 100/1 dynamic range, and its photocathode spectral response is required in a small package requiring low power. The high-light-level image quality of this camera is limited principally by its 244 x 248 pixel CID. When higher resolution CIDs are available they can also be used in similar LLLTV cameras.

REFERENCES

1 Riegler GR & More KA, IEEE Trans Nucl Sci NS-20,102 (1973)
2 Barton JB, Cuny JJ & Collins DR, Proc Int Conf CCDs, San Diego,133 (OCT 75)
3 Ceckowski DH, Proc Electro-Optics/Laser '76 Conf, 660 (OCT 76)
4 Lynch TF, Proc Electro-Optics/Laser '78 Conf, Boston, 78 (SEP 78)
5 Roetling PC & Ganley WP, J Opt Soc Am 52, 99 (1962)
6 Eberhardt EH, Appl Opt 18, 1418 (1979)
7 Lieber AJ, Rev Sci Instr 43, 104 (1972)
8 Lundy A, et al, IEEE Trans Nucl Sci NS-25, #1, 591 (1978)
9 Catchpole CE, Photoelectronic Imaging Devices 2, Plenum,NY,167(1971)
10 Lescovar B, Physics Today, 42 (NOV 77)
11 Eberhardt EH, Appl Opt 18, 1418 (1979)
12 Michon GJ & Burke HK, ISSCC Digital Techniques Papers, 138 (FEB 73)
13 Burke HK & Michon GJ, IEEE J Solid State Circuits SC-11, #1,121(1976)

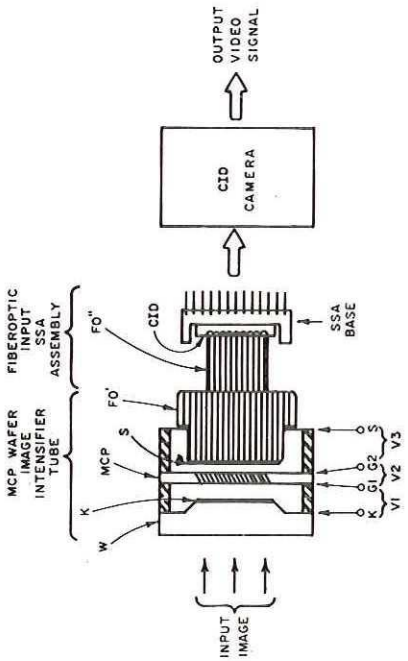

FIG. 1: ICID CAMERA GENERALIZED DESIGN

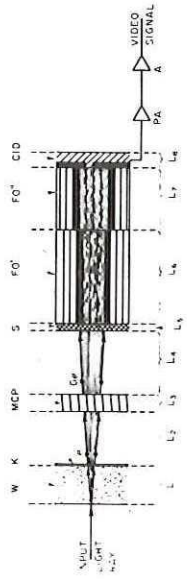

FIG. 2: ICID SCHEMATIC SIGNAL FLOW

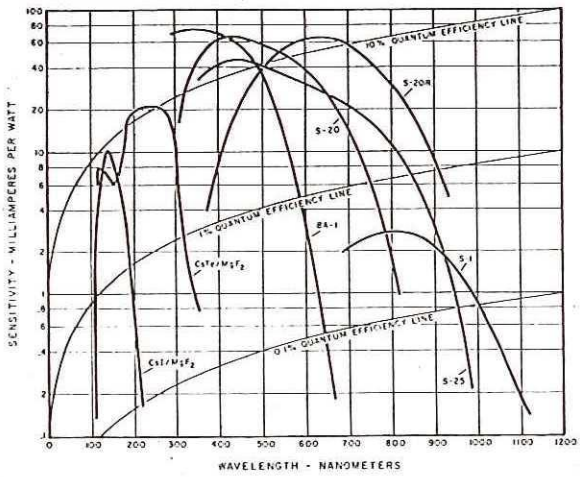

FIG. 3: PHOTOCATHODE SPECTRAL CHARACTERISTICS

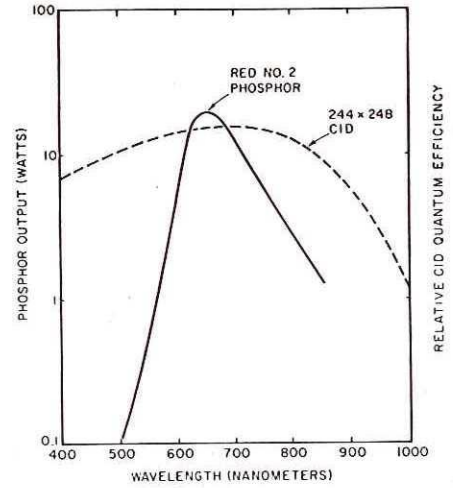

FIG. 4: PHOSPHOR AND CID SPECTRAL CHARACTERISTICS

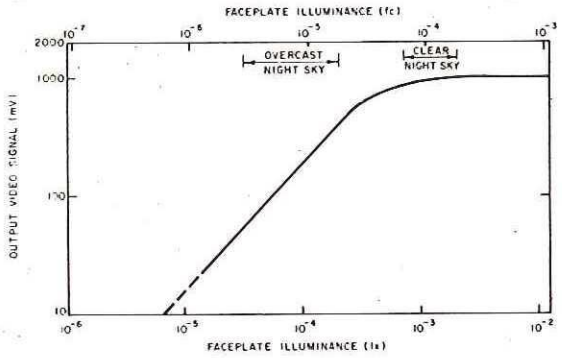

FIG. 5: ICID SIGNAL TRANSFER CHARACTERISTIC

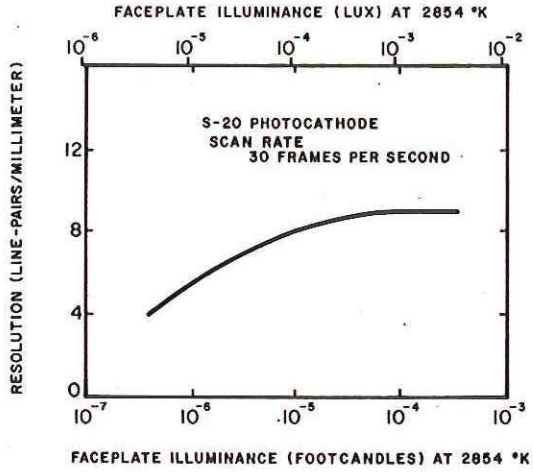

FIG. 6: ICID CAMERA ILLUMINANCE/ RESOLUTION CHARACTERISTIC

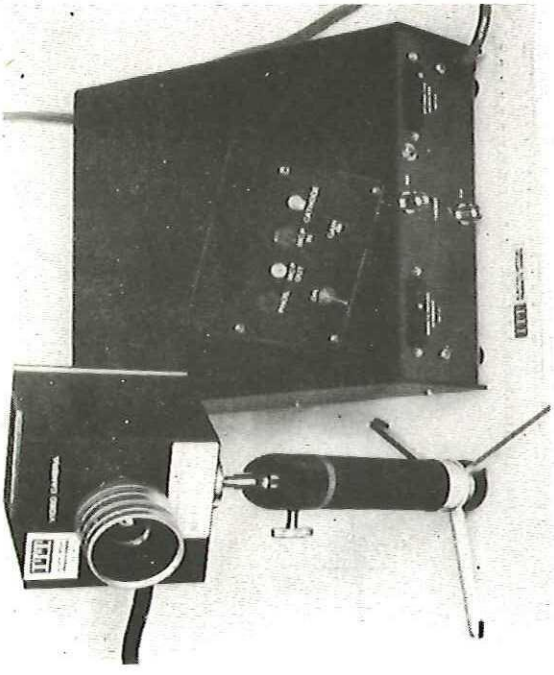

FIG. 7: ICID CAMERA

TABLE 1: SUMMARY OF THE MTFs OF THE IMAGE TRANSFER AND CONVERSION STAGES OF THE ICID

	STAGE	MTF (f, CYCLES/MM)	TYPICAL CONDITIONS: PARAMETER VALUES	MTFs
A	FIBEROPTIC INPUT WINDOW, OR GLASS INPUT WINDOW	$T_1(f) = \exp(-1.7D_1 f)^2$, or $T_1(f) \approx T(f)$	D_1 = 6 μm	$T_1(f) = \exp-(f/100)^2$, or $T_1(f) = 1$
B	CATHODE/MCP-ELECTRON OPTIC	$T_2(f) = \exp-(2\Pi L_2 f/(V_2/\bar{V}_{r2})^{1/2})^2$	V_2 = 180 V $\bar{V}_{r2}$ = 0.10 V L_2 = 0.25 mm	$T_2(f) = \exp-(f/26)^2$
C	MCP	$T_3(f) = \exp-(1.7D_3 f)^2$	D_3 = 12 μm	$T_3(f) = \exp-(f/49)^2$
D	MCP/SCREEN-ELECTRON OPTIC	$T_4(f) = \exp-(2\Pi L_4 f/(V_4/\bar{V}_{r4})^{1/2})^2$	V_4 = 5000 V $\bar{V}_{r4}$ = 0.25 V L_4 = 1.3 mm	$T_4(f) = \exp-(f/17)^2$
E	SCREEN	$T_5(f) = \exp-(f/f_{c5})^2$	f_{c5} = 45 cycles/mm	$T_5(f) = \exp-(f/45)^2$
F	TUBE FIEROPTIC	$T_6(f) = \exp-(1.7D_6 f)^2$	D_6 = 6 μm	$T_6(f) = \exp-(f/100)^2$
G	CID FIEROPTIC	$T_7(f) = \exp-(1.7D_7 f)^2$	D_7 = 6 μm	$T_7(f) = \exp-(f/100)^2$
H	CID	$T_8(f) = \text{sinc}(2\Pi D_8 f)$	D_8 = 36 μm, VERT D_8 = 46 μm, HOR	$T_8(f) = \text{sinc}(\Pi f/14)$, VERT $T_8(f) = \text{sinc}(\Pi f/11)$, HOR
I	TOTAL FOR GLASS INPUT WINDOW ICID CAMERA, WHERE $\prod_{n=1}^{n=7} T_n(f) = \exp-(f/13)^2$, AND $T(f) = \exp-(f/13)^2 T_8(f)$.			$T(f) = (\exp-(f/13)^2 \text{sinc}(\Pi f/14)$, VERT $T(f) = (\exp-(f/13)^2 \text{sinc}(\Pi f/11)$, HOR $T(12) = 0.07$, VERT; $T(10) = 0.05$, HOR